HEAT TRANSFER ANALYSIS OF LOOPED MICRO HEAT PIPES WITH GRAPHENE OXIDE NANOFLUID FOR LI-ION BATTERY

by

Manikanda Prabu NARAYANASAMY[a*], Sureshkannan GURUSAMY[a], Suresh SIVAN[b], and Senthilkumar A P[c]

[a] Department of Mechanical Engineering, Coimbatore Institute of Technology, Coimbatore, India
[b] Department of Mechanical Engineering, National Institute of Technology, Tiruchirappalli, India
[c] Department of Mechanical engineering, PSG College of Technology, Coimbatore, India

Original scientific paper
https://doi.org/10.2298/TSCI200125218M

Li-ion batteries play a vital role in electromechanical devices. The heat load on such batteries varies with time and application which falls as high temperature rise and it causes severe damages on a device and reduces the life cycle. It will be a big challenge in future decades of electronic devices and the electric car revolution. To overcome such difficulties, this work is considered for thermal management of small Li-ion batteries to check the possibilities through the micro heat pipe. Due to the high impact of nanotechnology in heat transfer science, acetone, deionized water, and tetrahydrofuran fluids are blended with graphene oxide nanoparticles to prepare the nanofluids by ultrasonic method. Here, tetrahydrofuran is a new combination of nanoworking fluid and not addressed by pre-researchers. Tetrahydrofuran-graphene nanofluid provides 61% of improved thermal conductivity than the other two fluids which accelerates the heat transfer rate with reduced thermal resistance in the range of 0.09-0.64 °C/W. To validate the experimental results, a real-time study has been done on Li-ion batteries for a day and ensured the reduction of overheat issues. Hence, the present work will support the Li-ion battery to work in an optimal temperature range in a new way of micro heat pipe with nanofluid.

Key words: *micro heat pipe, graphene oxide, enhancement heat transfer, nanofluid, energy storage*

Introduction

Li-ion battery is a familiar energy storage system in electric vehicles with several advantages of an improved life cycle, high energy density, superior capacity, and fast charging capability. But the operating temperature limits of this battery is optimized to 25-40 °C [1]. The development of electric vehicle technology has been internationally growing up due to the awareness spreads on low or zero-emission vehicles. Despite this, heat is a major battery killer and also lithium secondary cells need careful temperature control to optimum working conditions. Operating at high temperatures leads to the destruction of the cell, hence, heat is to be removed faster than it is generated and a thermal runaway may occur. An experimental loop is designed and tested with an air cooling system for Li-ion batteries to overcome this temperature rise [2]. Various research work on thermal management of battery pack is studied and different cooling methods have been proposed such as battery pack with air cooling [3-5], liquid cooling battery pack

* Corresponding author, e-mail: mkp.thetrinity@gmail.com

[6], and phase change materials (PCM) cooling [7, 8]. The performance difference between Air and liquid cooling also discussed in terms of basic flow and heat transfer parameters [9]. It is observed that the temperature directly reduces the performance and life span of batteries. Maintaining stable and uniformly distributed temperatures within the specified operating temperature range in all modules and battery cells is a major key factor to prolong the life of battery packs. The effects of the ventilation locations of the inlet, outlet, and the gap in battery cells are experimented [10]. An article highlighted the recent advances in thermal characterization and modeling of Li-ion batteries with an emphasis on the multi-scale aspect [11]. Despite numerous cooling techniques, heat pipes are recently being applied for thermal management of integrated electronic systems. The cooling capacity of a micro heat pipe is governed by the magnitude of capillary pressure induced in the wick structure [12]. Hence, this work considered to use the heat pipe as a cooling system. The maximum heat transport in moderate temperature applications is limited by the capillary pressure that can be generated by the wick structure [13]. The evaporator resistance depends on many parameters such as heat load, geometry of evaporator, porosity, and permeability of the wick, amount of the working fluid used [14]. The wicking and its evaporation characteristics of diverse wick micro-structures were experimentally investigated for heat transfer enhancement [15, 16]. In recent researches, nanotechnology plays a vital role in heat transfer applications which includes heat pipes also. The rapid improvement in electronic devices has led to an increased demand for effective cooling techniques. Many observations lead to the conclusion that heat enhancement is possible with nanofluids and it can be enhanced further in the presence of a high volume rate [17]. Experimental observations on nanofluids based heat pipes of various types such as micro-grooved heat pipes [18, 19], mesh wicked heat pipes [20], and sintered metal wicked heat pipes [21, 22] are observed. Various authors experimentally concluded the use of nanofluids instead of base fluids which led to a massive reduction in thermal resistance [23], the wall temperature [24, 25] and an increase in the thermal conductivity [26, 27] of the heat pipe is observed. Thermal conductivity and dynamic viscosity affected by the parameters such as volume fractions, base fluids type, and the base fluids temperature, and it was studied with artificial neural network for modeling the nanofluids [28]. An oscillating heat pipe with erythritol as PCM was tried and thermal performance was observed with 1-5 wt.% and 10-50 wt.%, the concentration of erythritol/water mixtures [29]. Here graphene oxide nanopowder is considered for fluid preparation. Graphene is an atomically thin sheet of hybridized carbon in 2-D form and honeycomb lattice structure have identified as an essential material in heat transfer applications due to its exceptional thermal transport properties [30]. Many studies reported the performance of cylindrical heat pipe, oscillating heat pipe, miniature heat pipes, grooved heat pipe and pulsating heat pipe using graphene-based nanofluids [31-35]. Also discussed on entropy generation and capillary limits in heat pipes [36, 37]. A detailed study of thermal properties of graphene in amide organic solvents showed an increase of thermal conductivity and specific heat on graphene integration with solvents [38]. Recent work used the graphene oxide in heat transfer of radiator with ethylene glycol as base fluid [39]. Normally, graphene with functional groups is called graphene oxide has better stability due to the strong bonding of hydrogen in water [40]. The thermal conductivity of graphene oxide is higher than familiar conductive materials like Cu and Al [41]. The graphene-oxide nanostructure and nanofluids have been considered as potential substitutes for water as heat transfer fluids in ground source heat pumps. Stability and transport properties like thermal conductivity and viscosity have been addressed as a function of temperature [42, 43]. The tendency of the particles in suspension to settle down concerning time is considered by two samples of the fluid and were put in two different measurement cuvettes. To identify the changes in sedimentation, the first sample was kept for thirty days and measured every day without shaking the fluid.

Similarly, the second sample is considered after the sonication of the fluid to monitor the changes in sedimentation [44]. From the literature survey, it is decided to select a model Li-ion battery, say a laptop battery to have practical experimentation with graphene nanofluids. Apart from existing base fluids such as deionized water and acetone, tetrahydrofuran is selected and the limitations of these fluids are discussed in accordance to application.

Materials and methods

The present work considered the looped micro heat pipe (LMHP) for experimentation. The LMHP was designed based on the 1-D steady-state model, fabricated and tested. Loop heat pipe (LHP) is an efficient two-phase heat transfer medium that uses the evaporation, condensation of a working fluid, and the capillary force developed in a fine porous wick [45]. The LHP has the capability of transferring heat over long distances and anti-gravity orientation. Electronics are quite a promising application of LHP [46]. Graphite is the base material of graphene oxide. The present work follows the Hummers-Offeman method which is a familiar method and practiced by pre-researchers to prepare graphene oxide [47]. The structural view of extracted graphene oxide is discussed in chapter *Experimental section*. The major properties of selected graphene oxide are given in tab. 1. Deionized water, tetrahydrofuran (THF), and acetone are the base liquids to prepare nanofluids. Taking deionized water as a familiar one, other liquids properties tabulated in tab. 1.

Table 1. Properties of selected materials

Graphene oxide		Acetone		Tetrahydrofuran
Appearance	Black/dark grey	Appearance	Colorless	Colorless
Thermal conductivity	2000-4000 W/mK	Density	0.79 g/cm^3	0.88 g/cm^3
Bonding energy	5.9 eV	Boiling point	55.8 °C	66 °C
Specific heat capacity	2.1 kJ/kgK	Viscosity	0.32 cP	0.45 cP
		Auto ignition	465 °C	478 °C

Preparation of nanofluids

It was noticed that graphene oxide could be dispersed in all kinds of engineering solvents except dichloromethane, n-hexane, methanol, and o-xylene. The stability of the various solvents with graphene oxide also experimentally investigated [48]. Two kinds of methods have been employed in producing nanofluids. One is a single-step method and the other is a two-step method [49]. Here, two-step method followed by using a high-frequency ultra-sonication method with 20 kHz and 700 W capacity. Base fluids of 50 mL are taken into ultra-probe and weight of 10% of nanoparticles are allowed to disperse inside liquids. Sodium dodecyl benzene sulfonate is served as a surfactant and sonication kept for four hours. After that, the homogeneous blend was taken in a beaker and subjected to zeta potential analysis for analyzing stability. To prepare graphene nanofluids using graphene oxide, oxygen-containing groups are introduced at the platelets surface during the preparation of graphene oxide which will improve the affinity of graphene with acetone and induces repulsive force between the nanolayers (hummers method). The filling ratio is a measure of the volume of working medium filled inside the heat pipe and it is assumed that a factor that influences the heat transportation characteristics. To calculate the filling ratio, the total volume of the micro heat pipe is estimated as V_t and input

volume V_i is assigned based on the volume of medium in terms of percentage like 15%, 30%, 45%, and 60%. The same is practiced while filling the nanofluids in the micro heat pipe. Mathematically, the filling ratio is expressed:

$$F_r = \frac{V_i}{V_t} 100 \tag{1}$$

Fabrication of micro heat pipe

A LMHP is selected for experimentation. The hydraulic diameter is the major parameter which ensures that, whether it is a micro-channel or not. So, the following specifications shown in tab. 2, were considered for fabrication. One end of the Cu tube is sealed carefully using brazing and another end is kept open for further work. High porous bronze metal wick is inserted in the compensating chamber of the heat pipe and pressure is maintained below the atmospheric level concerning nanofluids.

Table 2. Specifications of the micro heat pipe

Parameter	Evaporator section [mm]	Condenser section [mm]	Compensating chamber [mm]
Inner diameter	1.1	1.3	4.8
Outer diameter	1.6	1.7	5.5
Length	100	60	9

In heat pipes, the internal parameters of the wick highly affect the heat transfer characteristics of the wick structure. Here, permeability, K, effective pore radius, R, and porosity, ε, are considered as major parameters and calculated by:

$$R = \frac{2\sigma}{\Delta P} \tag{2}$$

$$\varepsilon = \frac{\frac{W_t - W_w}{\rho_l}}{\frac{W_w}{\rho_w}} 100 \tag{3}$$

$$K = \frac{d^2 \varepsilon^2}{122(1-\varepsilon^2)} \tag{4}$$

where W_t [kg] is the weight of saturated wick, W_w [kg] – the net weight of wick, ρ_l [kgm^{-3}] – the density of fluid, ρ_w [kgm^{-3}] – the density of wick, P [Nm^{-2}] – the pressure, and d [mm] – the pore diameter.

For fine bronze wick material, the porous radius is calculated as 1.3-1.9 μm, porosity as 71-80%, permeability is 1.2-2.75·10^{-12} m^2. Then the prepared nanofluid is poured into a micro heat pipe with a different filling ratio of 15%, 30%, 45%, and 60%. For each working fluid, four micro heat pipes fabricated by keeping different filling ratios.

Experimental section

Material characterization

The micro-structure and morphology of the graphene oxide nanoparticles were observed by SEM. This equipment is read the outcomes in terms of micrometer scale from the

magnification range of ×1000 to ×20000. Figure 1, indicates the SEM image of graphene oxide nanoparticles at ×1000 and ×5000, where the grain size and surface morphology were observed. The images of the graphene oxide have a well-defined shape and interlinked 3-D graphene sheets which form a porous network like loose sponge structure. Also it indicates that graphene oxide has a layered structure that makes homogeneous graphene films with micro-thin size. From this film, it is possible to distinguish the edges of individual graphene sheets with kinked and wrinkled areas. Structurally, the graphene oxide particles may resemble the graphene sheet because its base having a high affinity to water molecules which forms a clustered layer in water and other solvents. It allows being uniformly deposited and suspended in wide-ranging substrates in the form of thin films.

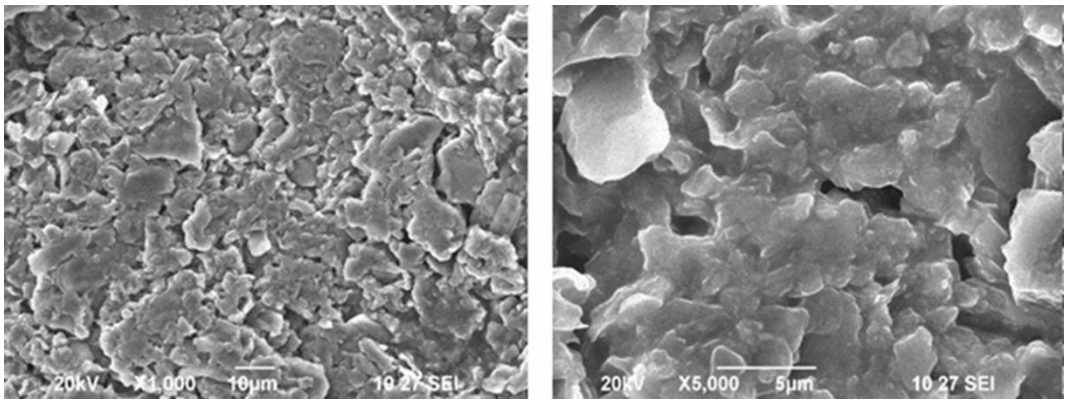

Figure 1. The SEM image of graphene oxide

Experimental set-up

A schematic line diagram of the micro heat pipe with an experimental set-up is shown in fig. 2. The micro heat pipe was placed horizontally on the heating source and cooling source. This was kept inside a temperature-controlled space with a size of 500 × 300 × 400 mm.

The temperature inside the controlled space was automatically controlled at 35±2 °C by a cooling fan equipped with a temperature sensor. The workspace is limited to 250 mm length and 150 mm wide where the heat pipe is set. The heating zone is covered with numerous cloth layers to overcome the heat losses which consists of a resistance heater to provide heating power to the micro heat pipe. The cooling section is exposed to the air-flow system by a small CPU fan. The evaporation section is considered lengthier than the condensation section which is shown in fig. 2.

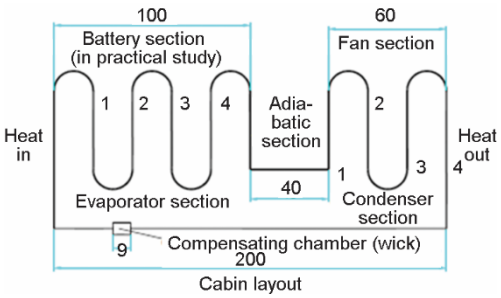

Figure 2. Experimental line diagram;
1, 2, 3, 4 – thermocouple points

Data loggers are used to monitoring the temperature from the thermocouple fixed at a uniform distance of 20 mm between each loop. These thermocouple measures the temperature at the outlet of each turn in the heat pipe. The thermocouples are calibrated in atmospheric pressure from 0-100 °C. All thermocouples used in this testing are *T*-type and diameter of

0.3 mm approximately with uncertainty measurement of 0.5-0.6 °C. The uncertainty of thermocouple, data loggers and thermal resistance are estimated as 0.00180, 0.0003, and 0.085 respectively.

Evaporator and condenser temperature

The temperatures on various points along the flow direction are observed on evaporator and condenser sections which ensure the measurement of thermal resistance characteristics, the minimum and maximum temperature range in the micro pipe system. Once the steady-state conditions reached, the LMHP becomes an isothermal heat conduction body and the temperature variation occurs in a very negligible range. Table 3 shows the sample of temperatures recorded on the LMHP with particular nanofluid before its attaining steady-state conditions.

Table 3. Temperature distribution of deionized water graphene oxice nanofluids at 10 W

Filling ratio [%]	Evaporator temperature [°C]				Condenser temperature [°C]			
	T_1	T_2	T_3	T_4	T_1	T_2	T_3	T_4
15	42.8	44	45.3	46.7	45.2	44.3	43	41.8
30	41	43	44.2	45	44	43.4	41.6	40.3
45	40	41	42.5	43.7	43.2	42.6	41	39.2
60	39.6	40.8	42	43	42.4	41	40.2	39

Results and discussion

Thermal resistance

The thermal resistance is a key factor of heat transfer from the evaporator to the condenser and it represents the heat-transfer capacity of the LMHP. It is related to the evaporator heat-transfer capacity and the condenser cooling efficiency:

$$R_{\mathrm{LMPH}} = \frac{T_{\mathrm{evaporator}} - T_{\mathrm{condenser}}}{Q_{\mathrm{input}}} \tag{5}$$

Therefore, the thermal resistance of the LHP can be reduced by improving the evaporator structure and the condenser cooling efficiency. The overall thermal resistance, LMHP, ranged from 0.21 °C/W to 1.34 °C/W, 0.14 °C/W to 1.10 °C/W, and 0.09 °C/W to 0.64 °C/W for deionized water, THF, and acetone, respectively. The minimum optimized resistance is obtained in 45% of the filling ratio. For heat loads more than 30 W, the temperature difference between the condenser inlet and outlet became less. It is also noticed that acetone is not providing uniform thermal resistance, it may due to low stability characteristics.

Effect of evaporator and condenser length

The evaporator section is subjected to a different heat load of 10 W, 30 W, and 50 W, respectively. The temperatures are recorded using data loggers which shows the variation with respect to the distance of fluid travel along the flow direction. Figure 3(a), indicates that evaporator temperature is increased concerning length along the flow path. Because the fluid from the condenser at a lower temperature is admitted to the evaporator section and flows inside at a particular distance by absorbing the heat energy from heat source. The boiling point is a major

parameter that enables the fast heating of fluids which reveals the reason for the high temperature of acetone and THF when compared to deionized water. Here, the variation in temperature at 10 W only considered for graphical representation and rest also providing the same structure. Similarly, in the condenser section, the hot fluid is exposed to the cooling fan which drastically reduces the temperature of the fluid. The number of loops in the condenser is less than the evaporator due to increased diameter. The fluid temperature has reduced along the distance shown in fig. 3(b). When compared to deionized water, acetone, and THF provides high condensate rate with respect to distance or number of loops on the condenser.

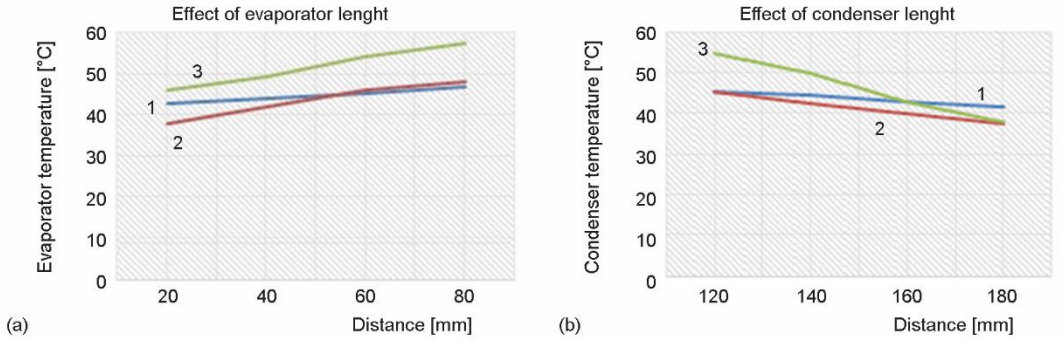

Figure 3. Temperature distribution along the length of (a) evaporator, (b) condenser; *1 – deonized, 2 – TMF, 3 – acetone*

Effect of fluid filling ratio

There is a small difference in temperatures at points 1-4 as tabulated in chapter *Evaporator and condenser temperature* and graphically mentioned in fig. 4. The fluid temperature at these points depends on the filling ratio and heat input. Figure 4 shows the condenser temperature with respect to various filling ratio.

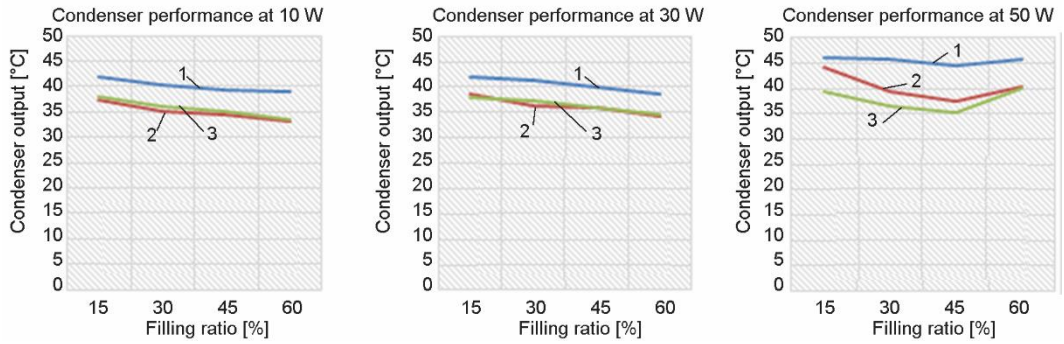

Figure 4. Effect of filling ratio on condenser performance; *1 – deonized, 2 – TMF, 3 – acetone*

It is observed that acetone and THF providing lower temperatures than deionized water at condenser due to the complete expansion during the fluid-flow. The condensate rate will depend on the volume of expansion of molecules and it gets poor in case of deionized water due to its high boiling point. Figure 5 shows the evaporator performance for various filling ratios. It is found that for minimum filling ratio the evaporator temperature is less at the inlet and increased further due to the expansion of molecules in the flow direction. At a high filling

ratio, the evaporator temperature is very less for the same heat input due to high volume flow at the entry of the evaporator section. The temperature is higher in acetone and THF compared with deionized water due to incomplete expansion since it has a high boiling point.

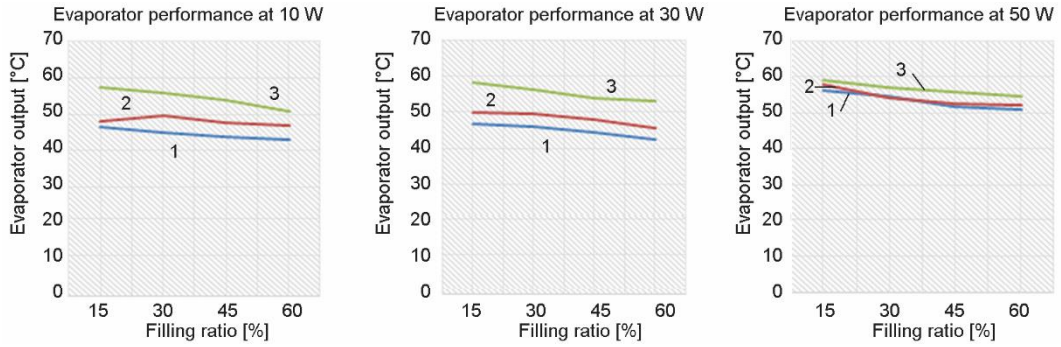

Figure 5. Effect of filling ratio on evaporator performance; *1 – deonized, 2 – TMF, 3 – acetone*

Stability of nanoparticles

Sedimentation is an easy and familiar method to check the stability used in many research articles. So the sedimentation method is tried by keeping the samples in different bottles for 14 days after ultra-sonication. The observations showed that acetone is not having greater miscibility with graphene oxide when compared to THF and deionized water. Figure 6(a), shows that, the stability of solvents in terms of the number of days in which they retained its stability. The same was reported as [48], THF has greater miscibility after keeping three weeks.

Effect of input power

Figure 6(b), reveals the effect of input power on the inlet temperature of the fluid. It is observed that, when the input power is increased, the entry temperature at the evaporator section is increased. For 10 W the inlet temperature will be less compared to the other two inputs. In addition to input power, filling ratio affects the inlet temperature.

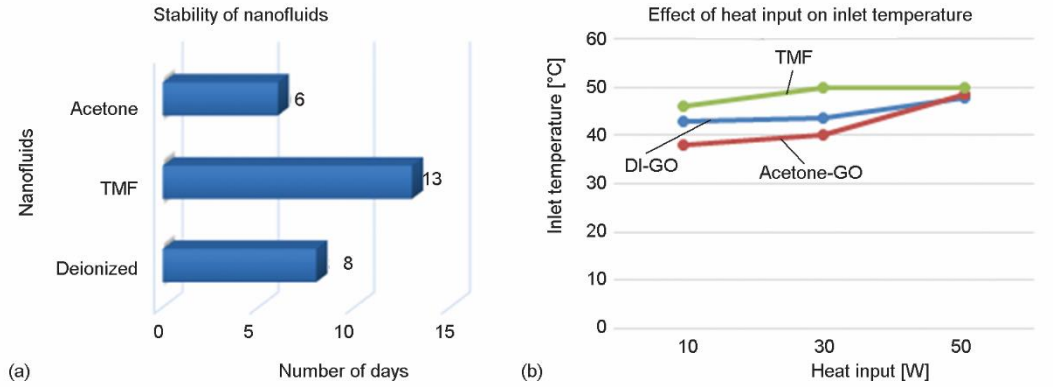

Figure 6. Stability of nanofluids (a), effect of input power (b); *GO – graphene oxide*

In the case of 30 W and 50 W, the entry temperature becomes high at a low filling ratio and it may cause damage in micro heat pipe because THF and acetone will exceed its boiling temperature. Hence, the various heat input with the increased filling ratio is examined.

The filling ratio of 30% and 45% are providing greater results at 10 W and 30 W input power due to the sufficient fluid and power to phase change at the condenser. For 10 W or 30 W with 60% filling ratio, it will have surplus fluid which tends to incomplete evaporation at the same pressure. But provides good results at maximum heat source like more than 50 W.

Conclusions

The complete experiment is successfully conducted and the following conclusions are suggested.

- Acetone graphene oxide nanofluid is providing greater performance than THF and deionized water nanofluids due to its low evaporation temperature and high condensation rate at normal temperatures. The maximum temperature difference obtained is 12 °C in acetone graphene oxide nanofluid which ensures the higher heat rejection from the system. But it may not suitable for the long term use for a particular application due to its lower stability character than THF and deionized water. When compared to deionized water graphene oxide nanofluid, THF graphene oxide is providing enhanced results in evaporation and condensation rate.
- The THF graphene nanofluid provides 61% of improved thermal conductivity than the other two fluids which accelerates the heat transfer rate along the flow direction with reduced thermal resistance in the range of 0.09-0.64 °C/W. Other nanofluids are having more thermal resistance of 0.21-1.34 °C/W and 0.14-1.10 °C/W.
- If the filling ratio is low, heat input will hit the walls of the heat pipe which causes damages on passage and super-heated phenomena take place. Hence the filling ratio is to be optimized before implementation. Here it is observed that 30% and 45% of filling ratio supports the current application to proper heat conductance.
- Stability is verified in both sedimentation and zeta potential method. Deionized water, acetone, and THF nanofluids are showing maximum zeta-value of 47 mV, 36 mV, and 53 mV, respectively. Hence THF attains better stability than the other two.
- Hence, this study recommending a new combination of THF graphene oxide as one of the acceptable working media to enhance heat transfer phenomena.
- A new scope in fluids of benzene, carbon tetrachloride, cyclohexane, and formic acid are identified to combine with graphene oxide as working medium to work out after having miscibility, stability, and toxic analysis.

Acknowledgment

The management of Presidency University, Bengaluru, India encourages this work to do better in all aspects.

Nomenclature

F_r – filling ratio
K – permeability, [m^2]
R – porous radius, [μm]
R_{LMHP} – thermal resistance of heat pipe, [°CW^{-1}]
V_i – input volume, [m^3]
V_t – total volume, [m^3]

Greek symbols

ε – porosity, [%]
σ – Stefan-Boltzman constant, [$Wm^{-2}K^{-4}$]

References

[1] Lip, H. S., *et al.*, Feasibility Study of Mist Cooling for Lithium-Ion Battery, *Energy Procedia, 142* (2017), 1, pp. 2592-2597

[2] Roberto, B. A., *et al.,* Air Cooling of Li-Ion Batteries: An Experimental Analysis, *Chemical Engineering Transactions, 57* (2017), 7, pp. 379-384
[3] Yang, N., *et al.*, Assessment of the Forced Air-Cooling Performance for Cylindrical Lithium-Ion Battery Packs: A Comparative Analysis between Aligned and Staggered Cell Arrangements, *Applied Thermal Engineering, 80* (2015), 1, pp. 55-65
[4] Sun, H., *et al,* Three-Dimensional Thermal Modeling of a Lithium-Ion Battery Pack, *Journal of Power Sources, 206* (2012), 10, pp. 349-356
[5] Sabbah, R., *et al.,* Active (Air-Cooled) vs. Passive (Phase Change Material) Thermal Management of High Power Lithium-Ion Packs: Limitation of Temperature Rise and Uniformity of Temperature Distribution, *Journal of Power Sources, 182* (2008), 2, pp. 630-638
[6] Valoen, L. O., Reimers, J. N., Transport Properties of LiPF6-Based Li-Ion Battery Electrolytes, *Journal of Electrochemical Society, 152* (2005), A, pp. 882-891
[7] Duan, X., Naterer, G. F., Heat Transfer in Phase Change Materials for Thermal Management of Electric Vehicle Battery Modules, *International Journal of Heat and Mass Transfer, 53* (2010), 23-24, pp. 5176-5182
[8] Kizilel, R., *et al.,* Passive Control of Temperature Excursion and Uniformity in High-Energy Li-Ion Battery Packs at High Current and Ambient Temperature, *Journal of Power Sources, 183* (2008), 1, pp. 370-375
[9] Taeyoung, H., *et al.,* Li-Ion Battery Pack Thermal Management-Liquid vs Air Cooling, *Journal of Thermal Science and Engineering Applications, 11* (2019), 2, ID 021009
[10] Hsiu, Y., Wang, H., *et al.,* Optimizing the Heat Dissipation of an Electric Vehicle Battery Pack, *Advances in Mechanical Engineering, 1* (2014), 1, pp. 1-25
[11] Rajath K., Amy, M. M., Heat Generation and Thermal Transport in Li-Ion Batteries – A Scale Bridging Perspective, *Nanoscale and Micro Scale Thermo-Physical Engineering, 23* (2014), 2, pp. 128-156
[12] Oh, K. H,., *et al.,* Design and Fabrication of a Metallic Micro-Heat Pipe Based on high-Aspect-Ratio Micro Channels, *Heat Transfer Engineering, 28* (2007), 8-9, pp. 772-778
[13] Kempersa, R., *et al.,* Characterization of Evaporator and Condenser Thermal Resistances of a Screen Mesh Wicked Heat Pipe, *International Journal of Heat and Mass Transfer, 51* (2008), 1, pp. 6039-6046
[14] Shwin, C. W., *et al.,* Evaporation Resistance Measurement with Visualization for Sintered Copper-Powder Evaporator in Operating Flat-Plate Heat Pipes, *International Journal of Heat and Mass Transfer, 53* (2010), 1-2, pp. 3792-3798
[15] Ranjan, R., *et al.,* Analysis of the Wicking and Thin-Film Evaporation Characteristics of Wick Microstructures, *ASME Journal of Heat Transfer, 131* (2009), 10, pp. 1-11
[16] Madhusree, K., Dey, T. K., Thermal Performance of Screen Mesh Wick Heat Pipes Using Water-Based Copper Nano Fluids, *Applied Thermal Engineering, 50* (2013), 1, pp. 763-770
[17] Saghir, M. Z., *et al.,* Experimental Measurements and Numerical Computation of Nano Heat Transfer Enhancement inside a Porous Material, *Journal of Thermal Science and Engineering Applications, 12* (2020), 1, pp. 011003
[18] Liu, Z. H., *et al.,* Thermal Performance of Inclined Grooved Heat Pipes Using Nanofluids, *International Journal of Thermal Sciences, 49* (2010), 9, pp. 1680-1687
[19] Do, K. H., Jang, S. H., Effect of Nanofluids on the Thermal Performance of a Flat Micro Heat Pipe with a Rectangular Grooved Wick, *International Journal of Heat Mass Transfer, 53* (2010), 9-10, pp. 2183-2192
[20] Liu, Z. H., Zhu, Q. Z., Application of Aqueous Nanofluids in a Horizontal Mesh Heat Pipe, *Energy Conversion Management, 52* (2011), 1, pp. 292-300
[21] Kang, S. W., *et al.,* Experimental Investigation of Nanofluids on Sintered Heat Pipe Thermal Performance, *Applied Thermal Engineering, 29* (2009), 5-6, pp. 973-979
[22] Riehl, R. R., Santos, N. D., Water Copper Nanofluid Application in an Open Loop Pulsating Heat Pipe, *Applied Thermal Engineering, 42* (2011), 1, pp. 6-10
[23] Wang, G. S., *et al.,* Operation Characteristics of Cylindrical Miniature Grooved Heat Pipe Using Aqueous CuO Nanofluids, *Experimental Thermal Fluid Science, 34* (2010), 8, pp. 1415-1421
[24] Saleh, R., *et al.,* Experimental Investigation of Thermal Conductivity and heat Pipe Thermal Performance of ZnO Nanofluids, *International Journal of Thermal Sciences, 63* (2013), 1, pp. 125-132
[25] Moraveji, M. K., Razvarz, S., Experimental Investigation of Aluminum Oxide Nanofluid on Heat Pipe Thermal Performance, *International Communication Heat Mass Transfer, 39* (2012), 9, pp. 1444-1448

[26] Asirvatham, L. G., *et al.*, Heat Transfer Performance of Screen Mesh Wick Heat Pipes Using Silver-Water Nanofluid, *International Journal of Heat Mass Transfer, 60* (2013), 1, pp. 201–209
[27] Hung, Y. H., *et al.*, Evaluation of the Thermal Performance of a Heat Pipe Using Alumina Nanofluids, *Experimental Thermal Fluid Sciences, 44* (2013), Jan., pp. 504-511
[28] Ghassan, F. S., Enhancement Heat Transfer of Cu-Water Nanofluids with Thermo Physical Properties Modeling by ANN, *Journal of Babylon University/Engineering Sciences, 25* (2017), 5, pp. 1721-1735
[29] Tingting, H., *et al.*, Experimental Investigation of Three-Phase Oscillating Heat Pipe, *Journal of Thermal Science and Engineering Applications, 11* (2019), 6, ID 061006
[30] Kamatchi, R., Kannan, K. G., An Aqua Based Reduced Graphene Oxide Nanofluids for Heat Transfer Applications: Synthesis, Characterization, Stability Analysis, and Thermo physical Properties, *International Journal of Renewable Energy Research, 8* (2018), 1, pp. 313-319
[31] Zhou, Y., *et al.*, Experimental Investigation of the Heat Transfer Performance of an Oscillating Heat Pipe with Graphene Nanofluids, *Journal of Powder Technology, 332* (2018), 1, pp. 371-380
[32] Sadeghinezhad, E., *et al.*, Experimental Investigation of the Effect of Graphene Nanofluids on Heat Pipe Thermal Performance, *Applied Thermal Engineering, 100* (2016), 1, pp. 775-787
[33] Tharayil, T., *et al.*, Thermal Performance of Miniature Loop Heat Pipe with Graphene Water Nanofluid, *International Journal of Heat and Mass Transfer, 93* (2016), Feb., pp. 957-968
[34] Mehrali, M., *et al.*, Effect of Nitrogen-Doped Graphene Nanofluid on the Thermal Performance of the Grooved Copper Heat Pipe, *Energy Conversation and Management, 118* (2016), 2, pp. 459-473
[35] Nazari, M. A., *et al.*, Experimental Investigation of Graphene Oxide Nanofluid on Heat Transfer Enhancement of Pulsating Heat Pipe, *International Communications in Heat and Mass Transfer, 91* (2018), Feb., pp. 90-94
[36] Tharayil, T., *et al.*, Entropy Generation Analysis of a Miniature Loop Heat Pipe with Graphene Water Nanofluid: Thermodynamics Model and Experimental Study, *International Journal of Heat and Mass Transfer, 106* (2017), Mar., pp. 407-421
[37] Kim, K. M., Bang, I. C., Effects of Graphene Oxide Nanofluids on Heat Pipe Performance and Capillary Limits, *International Journal of Thermal Science, 100* (2016), Feb., pp. 346-356
[38] Daniel, R. G., Maria del, R. R., From Thermal to Electro Active Graphene Nano fluids, *Energies, 12* (2019), 4545, pp. 1-11
[39] Babu, R. P., *et al.*, Heat Transfer Analysis of Radiator Using Graphene Oxide Nanofluids, *IOP conference series: Material Science and Engineering, 346* (2018), 28-29, pp. 1-8
[40] Kamatchi, R., *et al.*, Synthesis, Stability, Transport Properties and Surface Wettability of Reduced GO/Water Nanofluids, *International Journal of Thermal Sciences, 97* (2015), 2, pp. 17-25
[41] Kamatchi, S., *et al.*, Experimental Investigation and Mechanism of Critical Heat Flux Enhancement in Pool Boiling Heat Transfer with Nanofluids, *Heat and Mass Transfer, 52* (2015), 11, pp. 2357-2366
[42] Sun, B., *et al.*, Graphene Nanosheets as Cathode Catalysts for Lithium-Air Batteries with an Enhanced Electrochemical Performance, *Carbon, 50* (2012), 1, pp. 727-733
[43] Balandin, A. A., *et al.*, Superior Thermal Conductivity of Single-Layer Graphene, *Nano Letters, 8* (2008), 3, pp. 902-907
[44] Fedele, L., *et al.*, Experimental Stability Analysis of Different Water-Based Nanofluids, *Nanoscale Research Letters, 6* (2011), 11, pp. 300-306
[45] Launay, S., *et al.*, Parametric Analysis of Loop Heat Pipe Operation: A Literature Review, *International Journal of Thermal Sciences, 46* (2007), 7, pp. 621-636
[46] Vasiliey, L., *et al.*, Loop Heat Pipes for Cooling of High-Power Electronic Components, *International Journal of Heat Mass Transfer, 52* (2009), 1-2, pp. 301-308
[47] Won, C. O., Feng, J. Z., Preparation and Characterization of Graphene Oxide Reduced from a Mild Chemical Method, *Asian Journal of Chemistry, 23* (2011), 2, pp. 875-879
[48] Paredes, J. I., *et al.*, Graphene Oxide Dispersions in Organic Solvents, *Langmuir, 24* (2008), 19, pp.10560-10564
[49] Zhu, D., *et al.*, Dispersion Behavior and Thermal Conductivity Characteristics of Al_2O_3-H_2O Nanofluids, *Current Applied Physics, 9* (2009), 1, pp.131-139

Paper submitted: January 25, 2020
Paper revised: June 15, 2020
Paper accepted: July 8, 2020